crystals

MDPI

Article

Sintering Characteristics and Microwave Dielectric Properties of $BaTi_4O_9$ Ceramics with $CuO–TiO_2$ Addition

Haoxuan Guo [1], Peishu Zhu [1], Qingping Lin [1], Min Gao [1], Deping Tang [2] and Xinghua Zheng [1,*]

[1] Institute of Advanced Ceramics, College of Materials Science and Engineering, Fuzhou University, Fuzhou 350108, China
[2] College of Zijin Mining, Fuzhou University, Fuzhou 350108, China
* Correspondence: brook76@163.com

Abstract: Sintering characteristics, phase evolutions, microstructures, and microwave dielectric properties have been investigated for $BaTi_4O_9$ ceramics prepared by traditional low temperature sintering using $CuO–TiO_2$ (CT) additions as aids. The sintering temperature of $BaTi_4O_9$ ceramics was found to evidently reduce from 1350 °C to about 1100 °C with a very small amount of 0.5 wt% CT addition. When the CT addition increased to beyond 0.5 wt%, however, it was not expected to further lower the sintering temperature. Meantime, the secondary phases of $Ba_4Ti_{13}O_{30}$, $BaTiO_3$, and TiO_2 were observed in these $BaTi_4O_9$-based ceramics when the CT content was beyond 2 wt%. With the introduction of the CT addition, the permittivity (ε) had little enhancement, and the temperature coefficient of the resonant frequency (τ_f) was improved to near zero. The $BaTi_4O_9$ ceramics with 0.5 wt% CT additions, sintered at 1100 °C, exhibited excellent microwave dielectric properties, such as ε = 36.9, Q × f = 23100 GHz, and τ_f = 2.5 ppm/°C. In addition, the densification mechanism and variations of the microwave dielectric properties have also been discussed with the crystal phase and microstructure's evolution.

Keywords: sintering characteristics; microwave dielectric properties; $BaTi_4O_9$; $CuO–TiO_2$

Citation: Guo, H.; Zhu, P.; Lin, Q.; Gao, M.; Tang, D.; Zheng, X. Sintering Characteristics and Microwave Dielectric Properties of $BaTi_4O_9$ Ceramics with $CuO–TiO_2$ Addition. *Crystals* **2023**, *13*, 566. https://doi.org/10.3390/cryst13040566

Academic Editors: Wen Lei and Kaixin Song

Received: 9 March 2023
Revised: 21 March 2023
Accepted: 23 March 2023
Published: 27 March 2023

1. Introduction

In the past several decades, great attention has been paid to microwave dielectric ceramics due to their wide applications in mobile and satellite telecommunication systems. Generally, to meet the demands, suitable permittivity (ε), low dielectric loss, and near-zero temperature coefficients of resonate frequencies (τ_f) are required for these microwave dielectric ceramics [1–6] For application in base stations or satellite telecommunications, high Qf values, middle permittivity (25 < e < 50), and near zero t_f (−10 ppm/°C < t_f < 10 ppm/°C) are usually required in microwave dielectric ceramics [3]. A series of compounds with middle permittivity, such as $BaTi_4O_9$, $Ba_2Ti_9O_{20}$, $(Zr,Sn)TiO_4$, $Ba(Zn_{1/3}Nb_{2/3})O_3$, $CaTiO_3–NdAlO_3$, and $CaLa_4Ti_4O_{15}$ have been developed for practical applications [3–7]. Recently, some novel dielectric ceramics with middle permittivity have been explored [8–11]. Among these dielectric ceramics with middle permittivity, TiO_2-rich compounds of $BaTi_4O_9$ exhibit excellent microwave dielectric properties such as a middle permittivity of 37–39, a high Qf of 21,000–37,000 GHz, and near-zero temperature coefficients of 15 ppm/°C [6,7].

Recently, low temperature co-fired technologies have been developed to meet the demand of the miniaturization of microwave devices. Thus, the sintering temperatures of microwave dielectric ceramics need to match with the internal electrodes of Ag and Ag–Pd with a low melting point, which are required low temperature co-fired ceramics (LTCC). $BaTi_4O_9$ exhibits excellent microwave dielectric properties such as a middle permittivity of 37–39, a high Qf of 21,000–37,000 GHz, and near-zero temperature coefficients of 15 ppm/°C. However, its sintering temperature is as high as 1350 °C, which is too high for application in the field of LTCC. In addition, lowering the sintering temperature is helpful for energy saving. Therefore, it is interesting to lower the sintering temperature of $BaTi_4O_9$ microwave

dielectric ceramics. For application in the field of LTCC, considering energy savings, two methods are, usually, adopted to reduce the sintering temperatures of dielectric ceramics with high sintering temperatures. One is to prepare the ceramics derived from nano-powder. The other is the introduction of glass or oxides with low melting temperatures to liquid phase sintering. The latter method has often been adopted to lower the sintering temperature of microwave dielectric ceramics [12–16]. In addition, some advanced sintering methods such as cold sintering [17] and microwave sintering [18] have been adopted to prepare functional ceramics at low temperatures. Considering the economic, energy saving, and production efficiencies, liquid phase sintering is the most well-known approach for the low temperature sintering of microwave dielectric ceramics.

Some studies have reported on the low temperature sintering of $BaTi_4O_9$ ceramics. BaO–ZnO–B_2O_3, La_2O_3–B_2O_3–CaO, B–La–Mg–Ti–O, and B_2O_3–ZnO–La_2O_3 glass and $BaCuB_2O_5$ and BaB_2O_4 compounds have been adopted as sintering aids to reduce the sintering temperatures of $BaTi_4O_9$ ceramics [14–16,19–21]. As shown in Table 1, sintering temperatures can be significantly lowered from 1350 °C to about 900 °C. For example, after the introduction of 27.5 wt% BaO–ZnO–B_2O_3 glass, the sintering temperature of $BaTi_4O_9$-based ceramics is considerably decreased to 925 °C, and excellent microwave dielectric properties such as ε = 26.4, Q × f = 27,300 GHz, and τ_f = 3.3 ppm/°C are achieved [15]. Some examples of glass such as La_2O_3–B_2O_3–CaO and B–La–Mg–Ti–O are even added in at concentrations as high as 50–70 wt% [19,21]. As stated above, although these glasses or compounds can effectively reduce the sintering temperature of $BaTi_4O_9$ ceramics, high-content aids, for example, 20%, have often been added in order to reduce the sintering temperature. The consequent results are the deterioration of the microwave dielectric properties. One is the degradation of the Qf value, the other is that the temperature coefficient is not zero. Therefore, it is important and urgent to prepare high Qf values and near-zero temperature coefficient $BaTi_4O_9$ microwave dielectric ceramics with a small amount of sintering aid.

Table 1. Comparison of microwave dielectric properties of $BaTi_4O_9$ ceramics with different additions.

Addition	e	Qf (GHz)	τ_f (ppm/°C)	Ts (°C)	Ref.
27.5 wt% BaO–ZnO–B_2O_3 glass	26.4	27,300	3.3	925	[15]
0.34–4.47 vol% CuB_2O_4 and $BaCuB_2O_5$	36–40	13,000–21,000	20–40	925	[16]
70 wt% B–La–Mg–Ti–O glass	20.49	24,000	145	860	[19]
20 wt% B_2O_3–ZnO–La_2O_3 glass	27	~20,000	6.5	900	[20]
50 wt% La_2O_3–B_2O_3–CaO glass	26	8000	150	875	[21]
0.5 wt% CuO–TiO_2	37.0	23,100	2.5	1100	This work

CuO is a common sintering aid for dielectric ceramics [22]. However, CuO, sometimes, does not reduce the sintering temperature enough to meet well the demands of the LTCC. Thus, CuO-based binary sintering aids are investigated. In previous studies, e.g., [23–25], once TiO_2 was introduced to CuO, the liquid phase temperature reduced to the eutectic temperature of the CuO–TiO_2 binary system. After the investigation of details via differential scanning calorimetry (DSC) and thermogravimetric (TG) analysis, in conjunction with hot-stage microscopy, the eutectic temperature and composition of the CuO–TiO_2 system was certified as 1010 ± 10 °C and 83 CuO:17 TiO_2, respectively [23]. However, a computed eutectic temperature of 919 °C and a composition of 16.7 mol% TiO_2 at p_{O2} = 1 atm have been reported by Lu et al. [24] for the CuO–TiO_2 system, which is shown in Figure 1. Although there is little variation in eutectic temperature and composition in these investigations, the eutectic temperature was low enough to act as a sintering aid. Thus, CuO–TiO_2 may be a prospect sintering aid for microwave dielectric ceramics. In the present work, the eutectic composition of CuO–TiO_2 has been chosen as a sintering aid to lower the sintering temperature of $BaTi_4O_9$ microwave dielectric ceramics. The sintering behaviors, microstructures, and microwave dielectric properties of $BaTi_4O_9$ ceramics have been investigated in detail. Additionally, the sintering mechanisms and variations

of microwave dielectric properties have been also discussed with the crystal phase and microstructure's evolution.

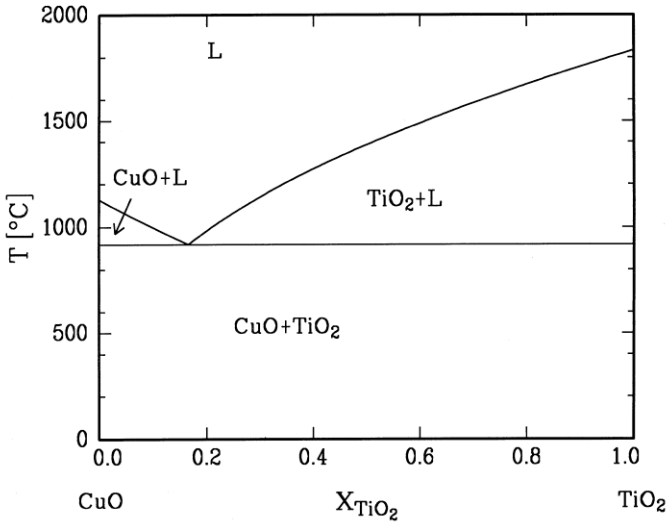

Figure 1. The calculated CuO–TiO_2 phase diagram at p_{O2} = 1 atm, as reported by Lu et al. [24]. The eutectic temperature and composition are 919 °C and 16.7 mol% TiO_2, respectively.

2. Materials and Methods

CuO–TiO_2 (CT) additions were prepared according to 83.3 mol% CuO-16.7 mol%TiO_2, using CuO (99.0%) and TiO_2 (99.0%) reagent powder. The weighted powder was ground for 12 h by ball milling in distilled water. Afterwards, the mixtures were dried to become a sintering additive. $BaTi_4O_9$ powder was synthesized by conventional solid-state reaction methods at a high temperature. According to the formula of $BaTi_4O_9$, raw materials of $BaCO_3$ (99.8%) and TiO_2 (99.0%) were weighed and ground in a polyethylene jar for 12 h by ball milling in distilled water. The ground powder was dried at 90 °C for 24 h and then calcined at 1200 °C for 2 h in air to obtain the single phase of the $BaTi_4O_9$. The calcined $BaTi_4O_9$ powder with a 0–10 wt% CT addition was reground for 8 h using distilled water. After drying, 5% PVA solution was added as a binder for granulation to the mixed powder. The granulated powder was pressed into pellets with a 13 mm diameter and a 2–6 mm thickness at a pressure of 100 MPa. To remove the PVA binder, the pellets were heated to 600 °C with a heating rate of 5 °C/min and a dwelling time of 2 h. After burning out the binder, the pellets were sintered in air by traditional liquid sintering at the temperature range of 1000–1125 °C with a dwelling time of 3 h to obtain the dense $BaTi_4O_9$-based ceramics. The heating rate was 5°C/min and cooled with the furnace after dwelling.

Thermogravimetry and differential thermal analysis (TG–DSC) were carried out by a synchronous thermal analyzer (STA 449C, NETZSCH, Germany), with a heating rate of 10 °C/min in an N_2 atmosphere from room temperature to 1150 °C. The bulk densities of the sintered samples were determined by the Archimedes method. The shrinkage (h) of the $BaTi_4O_9$-based ceramics was calculated from the diameter difference before and after sintering. The equation was $h = (r_0 - r_1)/m_0 \times 100\%$, where r_0 and r_1 were the diameters before and after sintering, respectively. The mass loss (d) of the pellets was evaluated by the mass difference before and after sintering, i.e., $d = (m_0 - m_1)/m_0 \times 100\%$, where m_0 and m_1 were the masses before and after sintering, respectively. The crystalline phases of the dense $BaTi_4O_9$-based ceramics were identified by powder X-ray diffraction (XRD, XD−5A, CuK_α, $\lambda = 1.5406 \times 10^{-10}$ m, Shimadzu, Japan). The polished and thermally etched surfaces of the sintered samples were observed by environmental scanning electron microscopy (ESEM, XL30 ESEM–TMP, Philips, Netherlands). Microwave dielectric properties of sintered samples were measured by the $TE_{01\delta}$ mode [26], using a vector network analyzer (R3767BH, Advantest, Japan). Additionally, the temperature coefficient of the resonant frequency τ_f was calculated from the temperature coefficient of the dielectric constant τ_ε,

according to the equation of $\tau_f = -1/2\tau_\varepsilon - \alpha$, where α was the linear expansion coefficient (~6–10 ppm/°C). τ_ε was measured in the temperature range of 25 to 85 °C using a precise LCR meter (Agilent 4284A, Agilent, Malaysia) at 1 MHz.

3. Results

Figure 2 shows the DSC and TG curves of $BaTi_4O_9$ powder with 0.5% and 5% CT additions as the function of temperature. As shown in Figure 1, an evident mass loss around 900 °C can be observed for $BaTi_4O_9$ powder with 0.5% CT, and a corresponding sharp endothermal peak appears in the DSC curve. This endothermal peak can be ascribed to the formation of the CuO–TiO_2 liquid phase, which is in agreement with the eutectic temperature of the CuO–TiO_2 binary reported by Lu et al. [24]. This is about 100 °C lower than the other reported values of eutectic temperatures in CuO–TiO_2 systems [23,25]. Although the CT addition is only 0.5%, the mass loss is as high as about 0.65%, which suggests that some $BaTi_4O_9$ dissolved into the eutectic liquid phase of the CuO–TiO_2 system. This is helpful for the densification of $BaTi_4O_9$ ceramics [27]. However, no evident mass loss is observed for the $BaTi_4O_9$ powder with a 5.0% CT addition when the temperature is beyond 800 °C. This is, evidently, different from that of the $BaTi_4O_9$ powder with a 0.5% CT addition. Furthermore, the corresponding endothermal peak becomes weak and wide in the DSC curve. The variation between the two DSC and TG curves for $BaTi_4O_9$ powder with 0.5% and 5% CT additions suggests that reaction occurs in the powders of the $BaTi_4O_9$ and CuO–TiO_2 addition, which results in the elevating of the liquid phase temperature. This results in no evident mass loss.

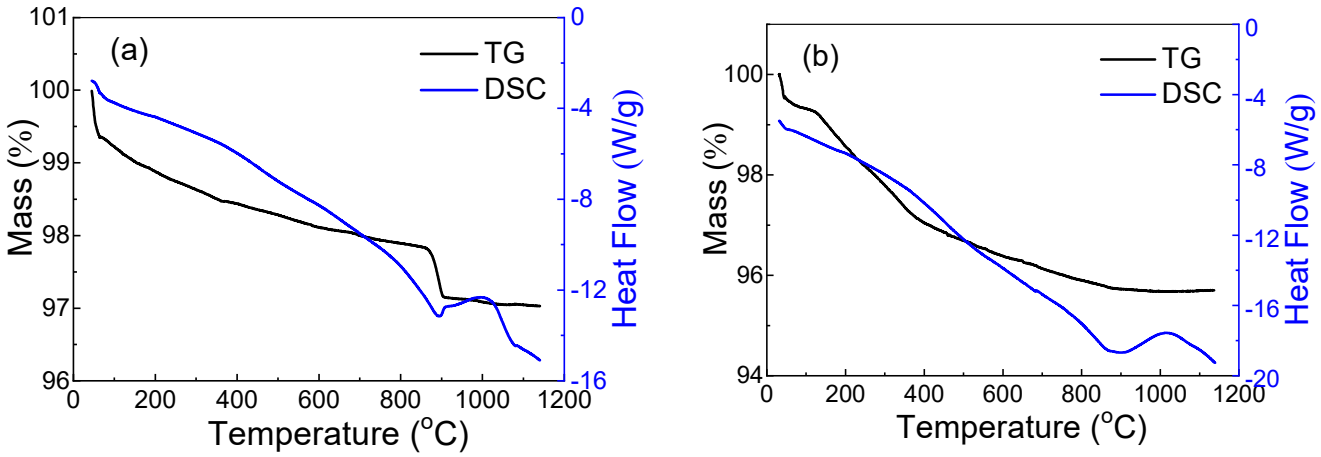

Figure 2. DSC and TGA curves of $BaTi_4O_9$ powder with (**a**) 0.5% and (**b**) 5.0% CT additions.

After sintering at different temperatures, the mass loss in Figure 3 is for the sintered $BaTi_4O_9$ ceramics with different contents of CT additions. The larger mass loss is observed for the $BaTi_4O_9$ ceramics with the higher CT addition. The mass loss is beyond 2.0% for the $BaTi_4O_9$ ceramics with a 10% CT addition. The mass loss is in the range of 0.55–0.85% for the $BaTi_4O_9$ ceramics with 0.5–5.0% CT addition. Although the dwelling time is 3 h and the sintering temperature is higher than eutectic temperature of CT, it should be noted that the value of mass loss is lower than the corresponding mass loss at a eutectic temperature of around 900 °C in the TG curve for $BaTi_4O_9$ powder with a 0.5 wt% CT addition. This is due to the N_2 atmosphere flow during the TG–DSC measurement. In addition, a low mass loss of 0.85% is observed for the $BaTi_4O_9$ ceramics with a 5.0% CT addition, which is also consistent with the result of the TG–DSC. For every $BaTi_4O_9$ ceramic with a different addition of CT content, four pellets are measured to evaluate the mass loss before and after sintering. The discrepancy of mass loss is below 0.025%.

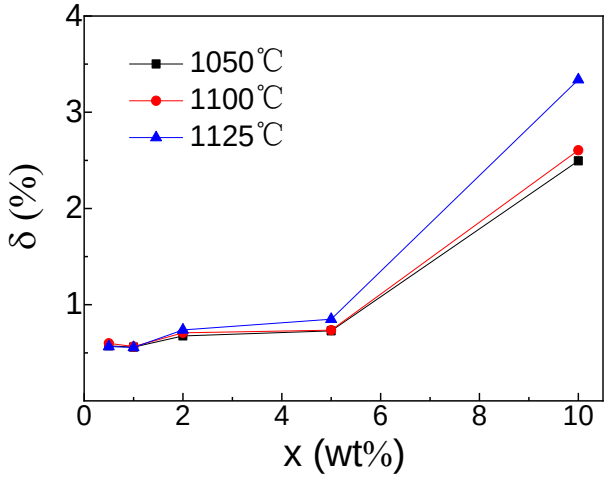

Figure 3. Mass loss of $BaTi_4O_9$ ceramics with different contents of CT additions, sintered at different temperatures.

The density (r) and shrinkage (h) of $BaTi_4O_9$ ceramics with various amounts of CT additions are shown in Figure 4. Without CT addition, pure $BaTi_4O_9$ ceramics are densely sintered at a high temperature of 1350 °C, which is consistent with previous reports [14,15]. After the introduction of a very small amount of CT (0.5%), the dense $BaTi_4O_9$-based ceramics with the density of about 4.4 g/cm^3 can be achieved at 1100 °C, which is evidently lower than the sintering temperature of 1350 °C for pure $BaTi_4O_9$ ceramics. However, with the increase in the CT addition, despite the density sintering at 1050 °C showing evident enhancements, the sintering temperature for the dense $BaTi_4O_9$-based ceramics is still around 1100 °C, which has little variation with the CT content. As shown in Figure 4a, similar trends of shrinkage are observed for the $BaTi_4O_9$-based ceramics with a CT addition. Additionally, the $BaTi_4O_9$ ceramics with a CT addition exhibit higher shrinkages, which are beyond 15%.

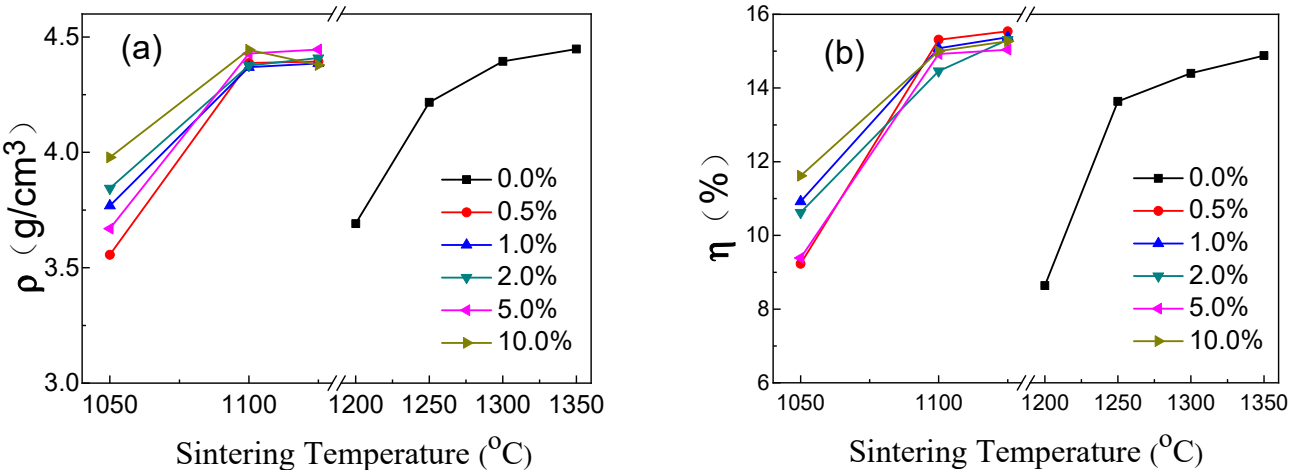

Figure 4. Densities (**a**) and shrinkages (**b**) of $BaTi_4O_9$ ceramics with different contents of CT additions.

Figure 5 demonstrates XRD patterns of dense $BaTi_4O_9$ ceramics with different contents of CT addition. According to the XRD patterns, all the diffraction peaks can be ascribed to the $BaTi_4O_9$ phase (JCPDS File No. 34-0070) for the $BaTi_4O_9$-based ceramics with a small amount of CT addition (below 2.0%). Otherwise, the secondary phases of $BaTiO_3$ (JCPDS File No. 05-0626), $Ba_4Ti_{13}O_{30}$ (JCPDS File No. 35-0750), and TiO_2 (JCPDS File No. 73-2224) are observed when the CT addition is above 2.0%. It has been reported that even a small deviation in $BaTi_4O_9$ can result in the formation of many stable TiO_2-rich compounds such as $Ba_4Ti_{13}O_{30}$ and $Ba_2Ti_9O_{20}$ in the BaO–TiO_2 system [28–30]. With increasing CT

additions, the intensities of the $Ba_4Ti_{13}O_{30}$ phase diffraction peaks are evidently enhanced, which indicates that the content of the $Ba_4Ti_{13}O_{30}$ phase gradually increases. When the CT content further increases to 10%, the $Ba_4Ti_{13}O_{30}$ phase becomes the major phase. This phase evolution may be due to the introduction of the CT to $BaTi_4O_9$. Combining the results of the TG–DSC and mass loss suggests that a partial reaction occurs between CT and $BaTi_4O_9$ during the sintering. When the temperature is elevated to a eutectic temperature of the $CuO–TiO_2$ system (around 900 °C), the liquid phase of the CT appears during the sintering. The CT liquid phase has two effects. One promotes the densification of $BaTi_4O_9$-based ceramics. The other induces the decomposition and partial dissolution of $BaTi_4O_9$ in the liquid phase because the Ti content of $Ba_4Ti_{13}O_{30}$ is lower than that of $BaTi_4O_9$. According to the phase evolution, the reaction equation can be depicted as follows,

$$4\ BaTi_4O_9 = Ba_4Ti_{13}O_{30} + 3\ TiO_2$$

$$BaTi_4O_9 = BaTiO_3 + 4\ TiO_2$$

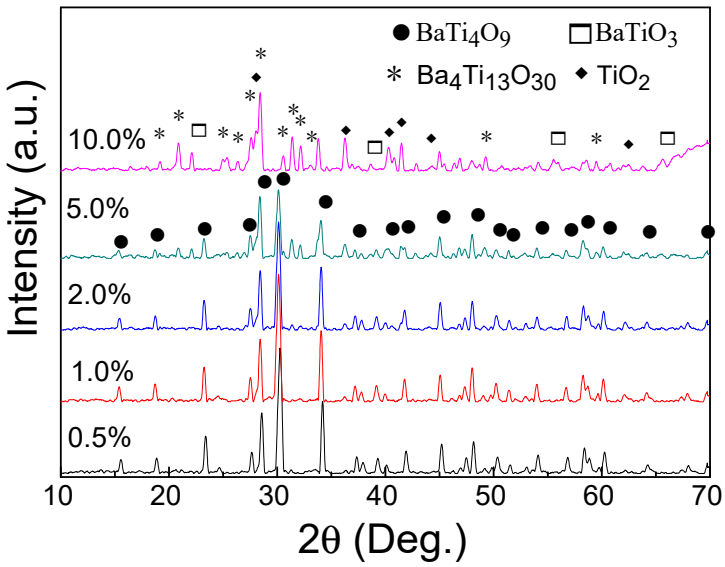

Figure 5. XRD patterns of dense $BaTi_4O_9$ ceramics with different contents of CT addition.

The decomposition of $BaTi_4O_9$ results in more TiO_2, which will increase the TiO_2 content of the $CuO–TiO_2$ system. Consequently, the composition of the CT addition is away from the eutectic composition, shifts to TiO_2, and ends in the $CuO–TiO_2$ system. This results in the temperature corresponding to the liquid phase of $CuO–TiO_2$ system rising and the noncongruent melting occurring, according to the theory of phase diagram. Therefore, a sharp endothermal peak and an evident mass loss are observed in the TG–DSC curves for $BaTi_4O_9$ powder with a 0.5% CT. However, no strong endothermal peak or evident mass loss are observed in the $BaTi_4O_9$ powder with a 5% CT addition. Thus, the sintering temperature of the $BaTi_4O_9$-based ceramics lowers to just around 1100 °C and does not further decrease when the CT addition further increases in the range of 0.5–10.0%. The sintering behaviors are closely related with the phase evolution.

Figure 6 gives SEM images of the dense $BaTi_4O_9$ ceramics with different amounts of CT additions. The present ceramics exhibit little porosity, which is consistent with the high densities in Figure 4a. After the introduction of the CT addition, the grains of $BaTi_4O_9$ ceramics are evidently smaller because the lower sintering temperature suppresses the grain growth. Additionally, some white regular grains in the $BaTi_4O_9$-based ceramics with a 1.0% or more CT addition clearly exist, and this content increases with the increase in the CT addition. Thus, this also certifies that partial reaction occurs between the CT and

$BaTi_4O_9$ during the sintering. These grains correspond to the secondary phases of $BaTiO_3$, $Ba_4Ti_{13}O_{30}$, and TiO_2. Additionally, there are a few grains with abnormal grain growths for the $BaTi_4O_9$-based ceramics with a 0.5% and 1.0% CT, as shown in Figure 5b,c. In addition, as shown in Figure 5e,f, melting phenomena are clearly observed for the $BaTi_4O_9$-based ceramics with a 5.0% and 10.0% CT. This indicates that more liquid phases are formed in the $BaTi_4O_9$-based ceramics during sintering.

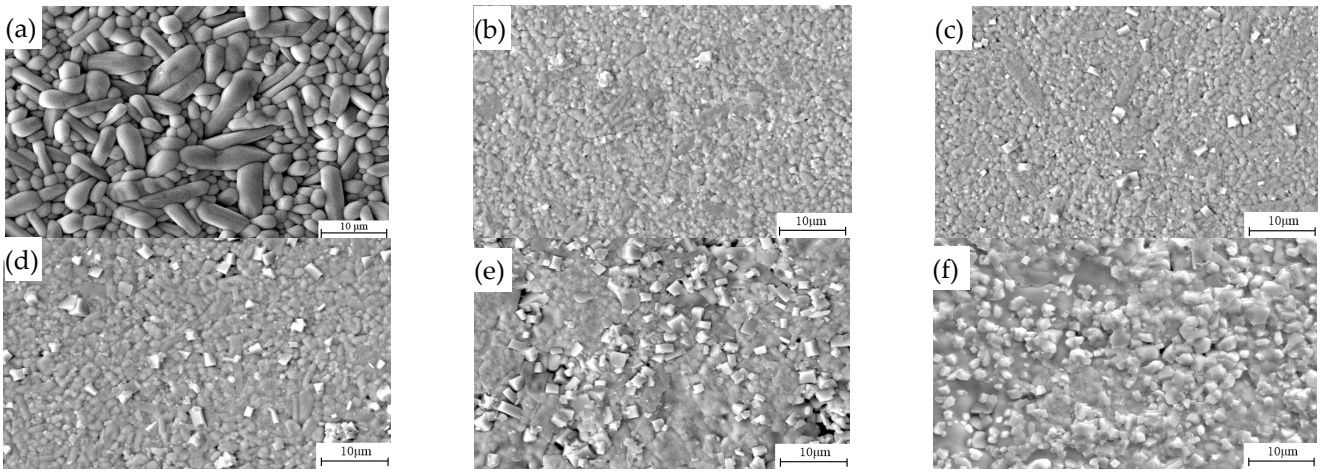

Figure 6. SEM images of $BaTi_4O_9$ dense ceramics with different CT additions, (**a**) 0%, (**b**) 0.5%, (**c**) 1.0%, (**d**) 2.0%, (**e**) 5.0%, (**f**) 10.0%.

From the variations in sintering behaviors and structure evolutions, the sintering mechanisms of $BaTi_4O_9$-based ceramics with CT additions can be concluded as follows. As per the TG–DSC results and the investigation of the $CuO–TiO_2$ system, the $BaTi_4O_9$-based ceramics with CT additions exhibit liquid phase sintering. According to the sintering theory of liquid phase sintering, the extensive densification of ceramics is associated with a low liquid solubility in solid combinations and a high solid solubility in the liquid [27]. When the temperature is elevated to the eutectic point of $CuO–TiO_2$, the liquid phase occurs during the sintering. As stated above, the sintering temperature of $BaTi_4O_9$ can be reduced from 1350 °C to about 1100°C with a very small amount of CT addition, e.g., 0.5%. In conclusion, $BaTi_4O_9$ has a high solid solubility in the liquid of $CuO–TiO_2$. XRD patterns demonstrate that the secondary phases of $BaTiO_3$, $Ba_4Ti_{13}O_{30}$, and TiO_2 are formed during sintering, which means that the decomposition of $BaTi_4O_9$ results in the formation of $BaTiO_3/Ba_4Ti_{13}O_{30}$ and TiO_2. Once the decomposition occurs, the content of TiO_2 increases. This results in composition shifts to the end of the rich TiO_2 in the $CuO–TiO_2$ system. Consequently, the liquid temperature rises and noncongruent melting occurs. Therefore, as shown in the TG–DSC curves, no strong endothermal peaks and evident mass losses are observed in the $BaTi_4O_9$ powder with a 5% CT addition. Thus, sintering temperature has little change with different contents of CT addition. However, more melting phenomena are observed in the SEM images for $BaTi_4O_9$-based ceramics with higher contents of CT addition.

As a function of CT additions, the microwave dielectric properties of $BaTi_4O_9$ ceramics are shown in Figure 7. With the increase in CT addition, permittivity keeps around 37.0 in the CT range of 0–1% and then elevates to 41.0 for a 10% CT addition. The permittivity of dielectric ceramics, in general, depends on the density and permittivity of constitution phases. As stated above, all of the $BaTi_4O_9$-based ceramics with CT additions have high densities. For the $BaTi_4O_9$-based ceramics with a small amount of CT addition (below 2.0%), only the $BaTi_4O_9$ phase is observed in the XRD patterns. Otherwise, the secondary phases of $BaTiO_3$, $Ba_4Ti_{13}O_{30}$, and TiO_2 with high permittivity are formed. Therefore, the variation in permittivity with CT addition is consistent with the phase evolution of $BaTi_4O_9$-based ceramics. However, there is a rapid decrease in the Qf values of the $BaTi_4O_9$

ceramics with a small amount of CT addition. When the CT addition is 10.0%, the Qf value rapidly deteriorates to below 10,000 GHz. This is likely because of the large amount of the $BaTiO_3$ and $Ba_4Ti_{13}O_{30}$ secondary phase with a high dielectric loss [16,28,31]. Compared to permittivity, there is an opposite trend for the temperature coefficient of the resonant frequency τ_f. The value of τ_f is around zero in the CT range of 0–1% and rapidly decreases when the CT addition is beyond 1%. Table 1 lists the microwave dielectric properties of some $BaTi_4O_9$-based ceramics sintered at low temperatures. Although previous studies studied sintering temperatures of only about 900 °C, there are two aspects that should be noted. One is that these investigations adopted larger content additions, such as 20%, which are far above that of the present work. The other is that the $BaTi_4O_9$-based ceramics exhibit low permittivity or high τ_f values. The excellent microwave dielectric properties of ε = 36.9, Q × f = 23,100 GHz, and τ_f = 2.5 ppm/°C are achieved for the $BaTi_4O_9$ ceramics sintered at 1100 °C with only a 0.5% CT addition.

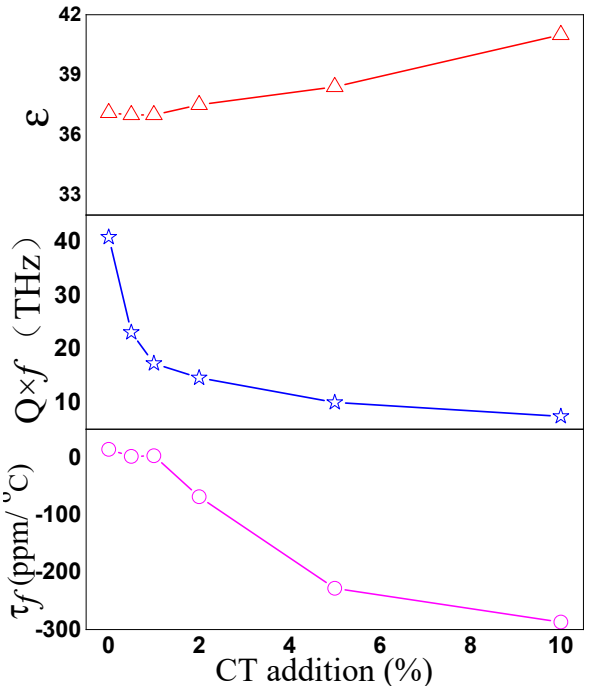

Figure 7. Microwave dielectric properties of $BaTi_4O_9$ ceramics with different content of CT addition.

4. Conclusions

The effects of the addition of CuO–TiO_2 (CT) on sintering behaviors, phase evolutions, microstructures, and microwave dielectric properties have been investigated for $BaTi_4O_9$ ceramics. The sintering temperatures of $BaTi_4O_9$ ceramics were found to evidently reduce from 1350 °C to about 1100 °C with a very small amount of CT addition, e.g., 0.5%. However, the sintering temperatures of $BaTi_4O_9$-based ceramics did not further decrease with the increase in CT addition. Furthermore, the secondary phases of $Ba_4Ti_{13}O_{30}$, $BaTiO_3$, and TiO_2 are observed in these $BaTi_4O_9$-based ceramics with a 2.0–10.0% CT addition. With a small amount of CT introduction, not only have the sintering behaviors been improved, but, also, the excellent microwave dielectric properties of ε = 36.9, Q × f = 23,100 GHz, and τ_f = 2.5 ppm/°C were achieved for the $BaTi_4O_9$ ceramics sintered at 1100 °C with a 0.5% CT addition. The variations in microwave dielectric properties and sintering mechanisms have also been discussed with TG–DSC, crystal phases, and microstructure evolutions.

Author Contributions: Conceptualization, M.G., D.T. and X.Z.; methodology, H.G.; formal analysis, P.Z. and Q.L.; resources, M.G., D.T. and X.Z.; writing—original draft preparation, H.G.; writing—review and editing, H.G. and X.Z. All authors have read and agreed to the published version of the manuscript.

Funding: The authors gratefully acknowledge the support of the National Natural Science Foundation of China (52102126) and the Natural Science Foundation of Fujian Province (2021J05123).

Data Availability Statement: The data and materials that support the findings of this study are available from the corresponding author upon reasonable request.

Conflicts of Interest: The authors declare no conflict of interest.

References

1. Sebastian, M.T.; Ubic, R.; Jantunen, H. Low-loss dielectric ceramic materials and their properties. *Int. Mater. Rev.* **2015**, *53*, 392–412. [CrossRef]
2. Lou, W.; Song, K.; Hussain, F.; Khesro, A.; Zhao, J.; Bafrooei, H.B.; Zhou, T.; Liu, B.; Mao, M.; Xu, K.; et al. Microwave dielectric properties of $Mg_{1.8}R_{0.2}Al_4Si_5O_{18}$ (R = Mg, Ca, Sr, Ba, Mn, Co, Ni, Cu, Zn) cordierite ceramics and their application for 5G microstrip patch antenna. *J. Eur. Ceram. Soc.* **2022**, *42*, 2254–2260. [CrossRef]
3. Reaney, I.M.; Iddles, D. Microwave dielectric ceramics for resonators and filters in mobile phone networks. *J. Am. Ceram. Soc.* **2006**, *89*, 2063–2072. [CrossRef]
4. Cao, X.X.; Wang, J.L.; Li, X.M.; Wu, X.; Zheng, X.H. Enhanced Sintering Behaviour and Microwave Dielectric Properties of $CaLa_4Ti_4O_{15}$ Ceramics with ZnO-B_2O_3 Addition. *Glass Phys. Chem.* **2019**, *45*, 126–132. [CrossRef]
5. Xiao, E.; Li, J.; Wang, J.; Xing, C.; Guo, M.; Qiao, H.; Dou, G.; Shi, F. Phonon characteristics and dielectric properties of $BaMoO_4$ ceramic. *J. Materiomics* **2018**, *4*, 383–389. [CrossRef]
6. Weng, M.H.; Liang, T.J.; Huang, C.L. Lowering of sintering temperature and microwave dielectric properties of $BaTi_4O_9$ ceramics prepared by the polymeric precursor method. *J. Eur. Ceram. Soc.* **2002**, *22*, 1693–1698. [CrossRef]
7. Ji, G.; Wang, J.; Bai, X.; Hao, M.; Chen, G.; He, J.; Fan, T.; Zhang, Z.; Chen, C.; Fu, C. Effects of MnO_2 and WO_3 co-doping and sintering temperature on microstructure, microwave dielectric properties of $Ba_2Ti_9O_{20}$ microwave ceramics. *Ceram. Int.* **2022**, *48*, 10713–10720. [CrossRef]
8. Xiao, E.; Cao, Z.; Li, J.; Li, X.H.; Liu, M.; Yue, Z.; Chen, Y.; Chen, G.; Song, K.; Zhou, H.; et al. Crystal structure, dielectric properties, and lattice vibrational characteristics of $LiNiPO_4$ ceramics sintered at different Temperatures. *J. Am. Ceram. Soc.* **2020**, *103*, 2528–2539. [CrossRef]
9. Liu, S.; Chen, X.; Zhang, P.; Wen, Q.; Ma, L.; Li, H. A novel microwave dielectric ceramic $La_5Sn_4O_{15}$ with medium-permittivity and low loss. *Ceram. Int.* **2023**, *49*, 95–100. [CrossRef]
10. Bao, J.; Guo, W.; Kimura, H.; Zhang, Y.; Du, J.; Zhou, Y.; Ma, Y.; Wu, H.; Yue, Z. Crystal structures, bond characteristics, and dielectric properties of novel middle-εr Ln_3NbO_7 (Ln=Nd, Sm) microwave dielectric ceramics with opposite temperature coefficients. *Ceram. Int.* **2022**, *48*, 36900–36907. [CrossRef]
11. Zhou, H.; Miao, Y.; Xu, J.; Gong, J.; Chen, X.; Fang, L. Novel middle permittivity ceramic $Ba_4CoTi_{11}O_{27}$: Sintering characteristic, cations distribution, crystal structure and microwave dielectric properties. *Ceram. Int.* **2015**, *41*, 5191–5195. [CrossRef]
12. An, Z.; Lv, J.; Wang, X.; Xu, Y.; Zhang, L.; Shi, F.; Guo, H.; Zhou, D.; Liu, B.; Song, K. Effects of LiF additive on crystal structures, lattice vibrational characteristics and dielectric properties of $CaWO_4$ microwave dielectric ceramics for LTCC applications. *Ceram. Int.* **2022**, *48*, 29929–29937. [CrossRef]
13. Yang, M.; Wei, S.; Su, S.; Chao, M.; Guo, J.; Wang, H.; Tang, X.; Jiao, Y.; Liang, E. The influence of $ZrMgMo_3O_{12}$ on the dielectric properties of $BaTi_4O_9$. *Ceram. Int.* **2020**, *46*, 10250–10255. [CrossRef]
14. Lü, X.; Lin, H. Investigation on low-temperature reactive viscous flow sintering behavior of lanthanum-borate glass-ceramic with $BaTi_4O_9$ ceramic filler. *J. Eur. Ceram. Soc.* **2020**, *40*, 4035–4046. [CrossRef]
15. Ren, H.; Xie, T.; Dang, M.; Jiang, S.; Lin, H.; Luo, L. Sintering mechanism and microwave dielectric properties of $BaTi_4O_9$-BBZ composite for LTCC technology. *Ceram. Int.* **2017**, *43*, 12863–12869. [CrossRef]
16. Chu, Y.J.; Jeann, J.H. Low-fire processing of microwave $BaTi_4O_9$ dielectric with crystalline CuB_2O_4 and $BaCuB_2O_5$ additives. *Ceram. Int.* **2013**, *39*, 5151–5158. [CrossRef]
17. Li, X.; Xue, X.; Lin, Q.; Qi, Z.; Wang, H.; Zhao, Y.; Guo, J. Cold sintered temperature stable xLi_2MoO_4-$(1-x)(LiBi)_{0.5}MoO_4$ microwave dielectric ceramics. *J. Eur. Ceram. Soc.* **2023**, *43*, 1477–1482. [CrossRef]
18. Nandihalli, N.; Gregory, D.H.; Mori, T. Energy-Saving Pathways for Thermoelectric Nanomaterial Synthesis: Hydrothermal/Solvothermal, Microwave-Assisted, Solution-Based, and Powder Processing. *Adv. Sci.* **2022**, *9*, 2106052. [CrossRef] [PubMed]
19. Ren, H.; Yao, X.; Xie, T.; Dang, M.; Peng, M.; Jiang, S.; Lin, H.; Luo, L. Low temperature sintering process, phase evolution and dielectric properties of $BaTi_4O_9$-filled B-La-Mg-Ti-O glass/ceramic composites. *J. Mater. Sci. Mater. Electron.* **2017**, *28*, 18646–18655. [CrossRef]
20. Guan, E.; Chen, W.; Luo, L. Low firing and microwave dielectric properties of $BaTi_4O_9$ with B_2O_3–ZnO–La_2O_3 glass addition. *Ceram. Int.* **2007**, *33*, 1145–1148. [CrossRef]
21. Wei, J.; Mao, H.; Zhang, W.; Shi, J. Study on low temperature sintering behavior and dielectric properties of $BaTi_4O_9/La_2O_3$-B_2O_3-CaO microwave dielectric ceramic. In Proceedings of the 2021 6th International Seminar on Advances in Materials Science and Engineering (ISAMSE 2021), Hangzhou, China, 13–15 August 2021; Volume 2021, p. 012082. [CrossRef]

22. Yu, S.Q.; Tang, B.; Zhang, X.; Zhang, S.R.; Zhou, X.H. Improved High-Q Microwave Dielectric Ceramics in CuO-Doped $BaTi_4O_9$–$BaZn_2Ti_4O_{11}$ System. *J. Am. Ceram. Soc.* **2012**, *95*, 1939–1943. [CrossRef]
23. Nie, J.; Chan, J.M.; Qin, M.; Zhou, N.; Luo, J. Liquid-like grain boundary complexion and sub-eutectic activated sintering in CuO-doped TiO_2. *Acta Mater.* **2017**, *130*, 329–338. [CrossRef]
24. Lu, F.H.; Fang, F.X.; Chen, Y.S. Eutectic reaction between copper oxide and titanium dioxide. *J. Eur. Ceram. Soc.* **2001**, *21*, 1093–1099. [CrossRef]
25. Rubia, M.A.; Reinosa, J.J.; Leret, P.; Romero, J.J.; Frutos, J.; Fernández, J.F. Experimental determination of the eutectic temperature in air of the CuO-TiO_2 pseudobinary system. *J. Eur. Ceram. Soc.* **2012**, *32*, 71–76. [CrossRef]
26. Fan, X.C.; Chen, X.M. Complex-permittivity measurement on high-Q materials via combined numerical approaches. *IEEE Trans. Microw. Theory Tech.* **2005**, *53*, 3130–3134. [CrossRef]
27. German, R.M. *Sintering Theory and Practice*, 2nd ed.; Wiley-Interscience: Hoboken, NJ, USA, 1996; pp. 226–227.
28. Luo, T.; He, L.; Yang, H.; Yu, H.; Yu, H. Phase evolution and microwave dielectric properties of $BaTi_4O_9$ ceramics prepared by reaction sintering method. *Int. J. Appl. Ceram. Soc.* **2019**, *16*, 146–151. [CrossRef]
29. Ren, H.; Xie, T.; Dang, M.; Yao, X.; Jiang, S.; Zhao, X.; Lin, H.; Luo, L. The influence of BBZ glass on phase evolution, sintering behavior and dielectric properties of $BaTi_4O_9$ ceramics. *J. Mater. Sci. Mater. Electron.* **2017**, *28*, 19090–19097. [CrossRef]
30. Zhang, J.; Yue, Z.; Luo, Y.; Zhang, X.; Li, L. Understanding the thermally stimulated relaxation and defect behavior of Ti-containing microwave dielectrics: A case study of $BaTi_4O_9$. *Mater. Des.* **2017**, *130*, 479–487. [CrossRef]
31. Templeton, A.; Wang, X.; Penn, S.J.; Webb, S.J.; Cohen, S.F.; Alford, N.M. Microwave Dielectric Loss of Titanium Oxide. *J. Am. Ceram. Soc.* **2000**, *83*, 95–100. [CrossRef]